



Hydrogen analysis and slow strain rate test in Ar gas for irradiated austenitic stainless steel

J. Morisawa^{a,*}, M. Kodama^a, N. Yokota^a, K. Nakata^b, K. Fukuya^c,
S. Shima^d, K. Asano^e

^a Research Department, Nippon Nuclear Fuel Development Co. Ltd., 2163 Narita-cho, Oarai machi, Ibaraki-ken 311-1313, Japan

^b The 2nd Materials Department, Hitachi Research Laboratory, Hitachi Ltd., 3-1-1 Saiwai-cho, Hitachi-shi, Ibaraki-ken 317-0073, Japan

^c Power and Industrial Systems, Research and Development Center, Toshiba Corp., 8 Shinsugita-cho, Isogo-ku, Yokohama, Kanagawa-ken 235-8523, Japan

^d Mechanical Technology and Design Department, Toshiba Corp., 8 Shinsugita-cho, Isogo-ku, Yokohama, Kanagawa-ken 235-8523, Japan

^e Materials Engineering Group, Power Engineering R&D Center, Tokyo Electric Power Company, 4-1 Egasaki-cho, Tsurumi-ku, Yokohama, Kanagawa-ken 230-8510, Japan

Received 17 September 2000; accepted 28 January 2001

Abstract

Hydrogen concentration in austenitic stainless steel irradiated with neutrons in boiling water reactors (BWRs) was measured and the effect of hydrogen in the austenitic stainless steel on intergranular cracking was investigated by the slow strain rate test (SSRT) in Ar gas. The hydrogen concentration decreased at low neutron fluences and increased at high neutron fluences. The decrease was attributed to the effect of heating or γ -ray irradiation at the early stage of reactor operation. The increase at high fluences was considered mainly due to the generation of hydrogen by nuclear transmutation. Intergranular cracking was not found for the specimen irradiated to a high fluence (1.4×10^{26} n/m²) in the SSRT at a very low strain rate (1.0×10^{-8} s⁻¹). This meant that the hydrogen concentration was too small to induce cracking, or hydrogen could not diffuse because of being trapped in irradiation defects at the test temperature. © 2001 Elsevier Science B.V. All rights reserved.

1. Introduction

Austenitic stainless steel irradiated in a boiling water reactor (BWR) has been reported to be sensitive to irradiation-assisted stress corrosion cracking (IASCC) [1–5]. The sensitivity depended on the neutron fluence and became higher with an increase of fluence [1,3,5]. For example, the sensitivity appeared at a fluence of 5×10^{24} n/m² ($E > 1$ MeV) or higher for Type 304 stainless steel [3–5]. Furthermore it was found that the

cracking by IASCC was caused by radiation-induced segregation such as the depletion of Cr and Mo, and the enrichment of P, S, Si and Ni in grain boundaries [6,7]. It was also reported that the sensitivity to intergranular cracking could be reduced by reducing the dissolved oxygen (DO) concentration for irradiated steel as well as unirradiated sensitized steels [1]. The depletion of Cr was assumed to be one of the key factors in the IASCC mechanism. However, even at a very low DO concentration where sensitivity to intergranular cracking disappeared for unirradiated and sensitized steel, intergranular cracking was induced and stress corrosion cracking (SCC) sensitivity was indicated for the irradiated steel. These results suggested that the sensitivity to intergranular cracking was due to hydrogen [8]. As the neutron fluence was increased, sensitivity to intergranular cracking by hydrogen appeared in irradiated steel [9]. The sources of hydrogen that affected the

* Corresponding author. Present address: Nuclear Systems Div., Nuclear Equipment Mfg. Department, Hitachi Ltd., 2-2 Omika-cho, 5 chome, Hitachi-shi, Ibaraki-ken 319-1221, Japan. Tel.: +81-294 28 1511; fax: +81-294 28 1671.

E-mail address: junichiro_morisawa@pis.hitachi.co.jp (J. Morisawa).

intergranular cracking of steel were considered to be the hydrogen in the steel itself and in the water environment. This paper focuses on the hydrogen in the steel. The purposes of this work are to measure hydrogen concentration in the steel, and to investigate the effect of hydrogen in steel on the sensitivity of intergranular cracking as investigated by the slow strain rate test (SSRT) in inert Ar gas. The results of this experiment are compared with the previously reported results of SSRTs in Ar gas for the steel irradiated in a pressurized water reactor (PWR) [10].

2. Experimental procedure

2.1. Materials

Test samples were Type 304 stainless steel pipe irradiated in a BWR. The dimensions of this steel pipe were 16 mm outside diameter (o.d.), and 1, 1.24, 1.5 or 2.3 mm thicknesses. The chemical composition, mechanical properties and neutron fluence are shown in Table 1. Neutron fluences ranged from 8×10^{23} to 1.4×10^{26} n/m². These samples had been irradiated for 1–7 yr in the reactor and then stored under water in the pool of the power station for 7–10 yr after removal from the reactor. The neutron fluence for each sample was calculated for its position in the reactor core and the operation history of the reactor. The as-received (AR) and heat-treated (in vacuum, 561 K \times 24 h and 561 K \times 72 h) samples of unirradiated Type 304 stainless steel Heats (A) and (B) were used as references for comparison with the irradiated samples.

2.2. Hydrogen analysis

Hydrogen was analyzed with an RH404 hydrogen analyzer (LECO, USA). The dimensions of specimens prepared for the hydrogen analysis were 6 mm wide \times 10 mm long (weight: about 0.5 g). A flow diagram of the hydrogen analyzer is shown in Fig. 1. The specimen was melted in a pulse furnace filled with Ar gas. The emitted gas, after removal of carbon dioxide and moisture, was separated into hydrogen and nitrogen in a column and the hydrogen was analyzed using a thermal conductivity detector. In order to facilitate hydrogen analysis in a hot cell, the system was modified by employing automatic sample recovery, and the number of parts in the hot cell was reduced by separating the stabilized power supply, controller, extraction part and detector. When irradiated samples were analyzed, the extraction and detector were installed in the hot cell and the stabilized power supply and controller were installed in the operation room (outside of the hot cell). The inside of the hot cell and operation room were connected

Table 1
Chemical composition, mechanical properties and neutron fluence in the materials

Materials	Dimensions (mm)	Chemical composition (at.%) ^a								Mechanical properties ^a		Neutron fluence (n/m ² , E > 1 MeV)
		C	Si	Mn	P	S	Cr	Ni	N ^b	Tensile strength (MPa)	Elongation (%)	
Type 304 Heat (A)	$\varnothing 16 \times 1.5t$	0.23	1.04	1.64	0.046	0.010	19.64	8.61	0.07	591	62.7	0.80×10^{23} to 9.7×10^{24}
Heat (B)	$\varnothing 16 \times 1t$	0.27	0.96	1.74	0.060	0.022	19.54	8.75	0.12	596	63.4	0.10×10^{24} to 1.03×10^{25}
Heat (C)	$\varnothing 19.05 \times 1.24t$	0.23	1.00	1.69	0.051	0.012	19.71	9.55	0.07	623	55	4.6×10^{25} to 6.0×10^{25}
Heat (D)	$\varnothing 17.3 \times 2.3t$	0.05	0.37	1.75	0.030	0.014	18.14	9.03	–	608	57.0	8.0×10^{25} , 1.4×10^{26}

^a Mill sheet.

^b Analyzed.

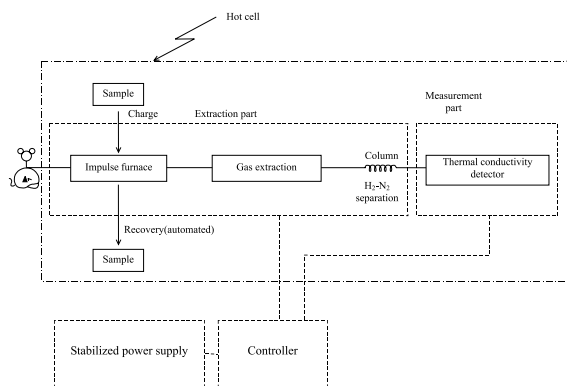


Fig. 1. Hydrogen analysis apparatus flow diagram.

with gas pipes and electric cables, and analysis was performed remotely from the operation room. The measurement error of this apparatus was within $\pm 11\%$ after the calibration by using the standard specimen.

Some of the difficulties in analyzing hydrogen in irradiated steel using this apparatus are as follows. When austenitic stainless steel is irradiated by neutrons in a reactor, hydrogen and helium are generated as gaseous elements. Nickel and nitrogen, which are constituents of the steel, are transmuted by the irradiation of fast neutrons and hydrogen is generated [11]. The generation rate depends on the fluence of fast neutrons. The irradiation of Ni with thermal neutrons generates He by two steps [12] and the rate depends on the thermal neutron fluence. The major reactions of generating protons (hydrogen) are given by the reaction of $^{58}\text{Ni}(n, p) ^{58}\text{Co}$, and $^{12}\text{N}(n, p) ^{12}\text{C}$, etc. [11], whereas those for helium are by the reaction of $^{58}\text{Ni}(n, \gamma) ^{59}\text{Ni}(n, \alpha) ^{56}\text{Fe}$ [12]. In this reaction ^{58}Ni is transmuted to ^{59}Ni by absorbing neutrons and emitting γ -rays in the first step, and then ^{59}Ni is transmuted to ^{56}Fe by absorbing neutrons and emitting α particles (He). Accordingly irradiated Type 304 stainless steel contains both hydrogen and helium.

Hydrogen and helium cannot be analyzed separately with this hydrogen analyzer, because there is little difference in thermal conductivity between hydrogen and helium [13] which is the basis of their analyses.

The measured data of helium content for the irradiated specimens used in this work have been published [14]. The procedure for measuring helium content was given in such a way that the number of thermally released ^4He atoms was counted by mass spectroscopy [15].

The helium concentrations are plotted as a function of fast neutron fluence in Fig. 2. The concentration of He increased at neutron fluences of $1 \times 10^{25} \text{ n/m}^2$ or higher. The helium concentration at each neutron flu-

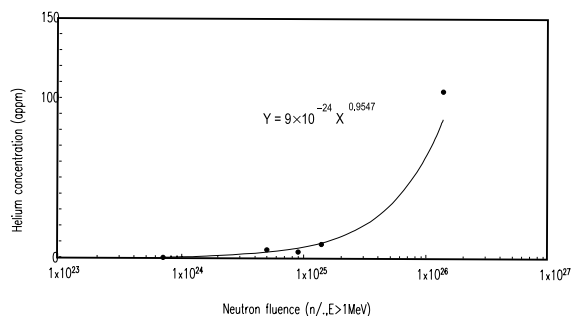


Fig. 2. Fast neutron fluence dependence of measured helium concentrations in Type 304 stainless steel (based on [14]).

ence was estimated from the figure, assuming that the ratio of fast neutrons and thermal neutrons was constant since these samples were irradiated in the same type of reactor (a BWR). The hydrogen concentration was also estimated by subtracting the helium concentration from the apparent hydrogen concentration, which is the sum of the hydrogen concentration and helium concentration obtained in this experiment. The helium concentration (C appm) to be subtracted must be doubled ($2 \times C$ appm) because the analytical value of this analyzer for hydrogen (H_2 , one molecule with two atoms) counts one molecule of He as having two atoms, though He is monoatomic.

2.3. SSRTs in Ar gas

Specimens for SSRTs in Ar gas were prepared using a milling machine in the hot cell by remote operation. The shape and dimensions are shown in Fig. 3. The SSRTs were carried out with an SSRT apparatus installed in the hot cell as shown in Fig. 4. The specimens were heated to 561 K in Ar gas after mounting in the apparatus for the SSRT. Three different strain rates, namely 2.5×10^{-7} , 5.0×10^{-8} and $1.0 \times 10^{-8} \text{ s}^{-1}$ were selected. The fractured specimens were observed by scanning electron microscopy (SEM) to inspect the fracture modes and the percentage of intergranular (%IG) cracking after the SSRT.

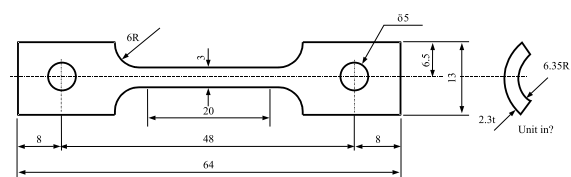


Fig. 3. Specimen shape and dimensions for SSRT.

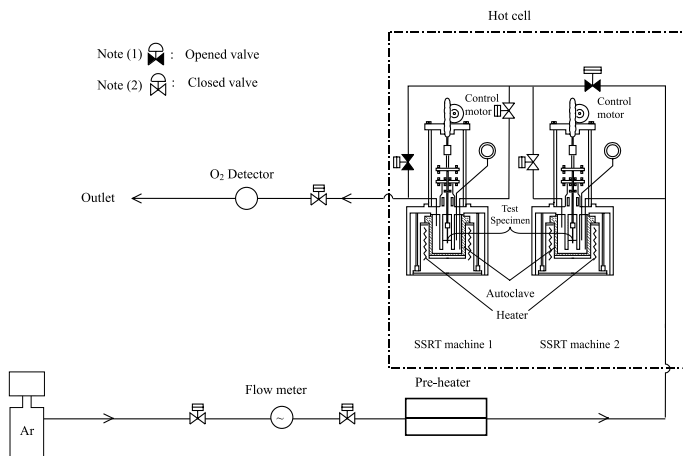


Fig. 4. SSRT apparatus system diagram (under Ar gas atmosphere).

3. Results and discussion

3.1. Hydrogen concentrations in unirradiated stainless steel

The hydrogen concentrations in unirradiated AR Type 304 stainless steel and heat-treated Type 304 stainless steel are shown in Table 2. In the AR condition, the average hydrogen concentration in Heat (A) was 215 appm which was higher than that in Heat (B). A hydrogen concentration of 275 appm for unirradiated Type 304 stainless steel has been reported [2]. The results of this experiment were comparable to that in the reference for unirradiated, AR steel.

Regarding the average hydrogen concentrations after heat treatment at 561 K × 24 h, 76% of the hydrogen

concentration for Heat (A) and 54% for Heat (B) were released, resulting in 52 and 73 appm, respectively. As a result, the hydrogen concentration in Heat (A) was lower than in Heat (B). The results after 72 h of heating, 53 appm for Heat (A) and 74 appm for Heat (B), were the same as the results after 24 h of heating. This meant that almost all hydrogen released at 561 K was released during the first 24 h of heating, and hydrogen diffused faster in Heat (A) than in Heat (B). The difference between Heat (A) and Heat (B) was assumed to be due to the difference in the solubility and diffusivity of hydrogen in steel due to the difference of trap sites in steel. The different nature of the trapping sites, which are precipitates of P and Cr carbide, etc. [16], was probably due to a difference in manufacturing processes.

3.2. Hydrogen concentrations in irradiated stainless steel

The relationship of apparent hydrogen concentration, which is the sum of hydrogen concentration and helium concentration, to neutron fluence in irradiated Type 304 stainless steel is shown in Fig. 5. The apparent hydrogen concentration included both hydrogen and helium as mentioned in the hydrogen analysis method in

Table 2
Hydrogen concentrations of unirradiated Type 304 SS

Materials		AR (appm)	Heat treatment conditions	
			561 K × 24 h	561 K × 72 h
Type 304 Heat (A)	Measured value	175	52	48
		232	51	58
		235		
		186		
	Average	215	52	53
Type 304 Heat (B)	Measured value	118	78	77
		164	68	71
		227		
		116		
	Average	161	73	74

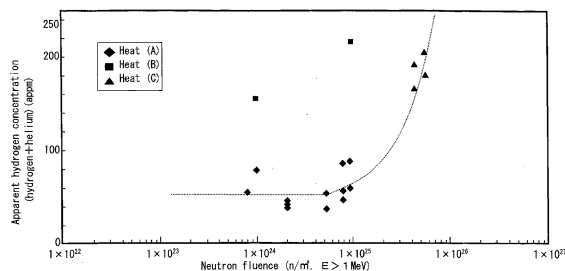


Fig. 5. Apparent hydrogen concentration (hydrogen + helium) in irradiated Type 304 stainless steel.

Section 2.2. The hydrogen concentration was obtained by subtracting the helium concentration from the apparent hydrogen concentration at each corresponding neutron fluence. The results are shown in Fig. 6. The hydrogen concentration indicated a neutron fluence dependency at the fluence of 5×10^{24} n/m² ($E > 1$ MeV) or higher and increased with the increase of neutron fluence. In order to investigate the reason for this, hydrogen generated by nuclear transmutation was calculated (calculated hydrogen generation). It was obtained using the ORIGEN-2 code [17] based on the chemical composition in Table 1 and neutron fluence. The neutron absorption cross-section used was that prepared in the ORIGEN-2 code. These results, and the relation between average hydrogen concentration and neutron fluence are shown in Fig. 7.

There was a difference in the tendency of increase in Heats (A) and (C), and Heat (B). The hydrogen concentration in Heats (A) and (C) is discussed first. The hydrogen concentration (about 30 appm) at a low neutron fluence of 8.4×10^{23} n/m² was lower than 215 appm of unirradiated steel and AR steel. The reason is considered to be as follows. The hydrogen content at first was decreased by the release due to the double effects of heating at 561 K at the early stage of operation and γ irradiation [18], and it became lower than that of the unirradiated steel heat-treated at 561 K \times 72 h. Thereafter, the hydrogen concentration increased with the increase of neutron fluence and reached about 110 appm at a high neutron fluence of 6×10^{25} n/m².

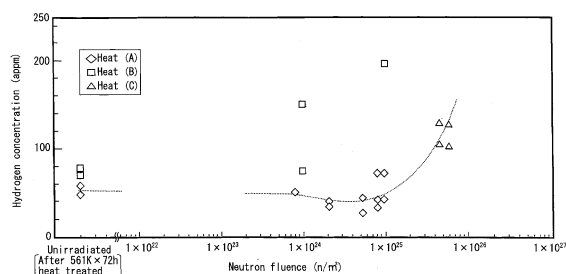


Fig. 6. Hydrogen concentration in Type 304 stainless steel.

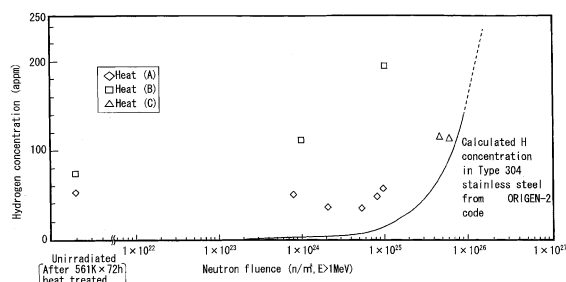


Fig. 7. Comparison of measured and calculated hydrogen concentrations.

The calculated hydrogen generation began to increase at the neutron fluence of 1×10^{24} n/m² and increased exponentially with the increase of neutron fluence. The Type 304 stainless steel Heats (A) and (C) showed the same tendency as the calculated hydrogen generation. The calculated hydrogen generation increased and the radiation-induced defects (twin and point defects, dislocation and dislocation loops), which functioned as hydrogen trap sites, increased with the increase of fluence [19]. Accordingly, the calculated hydrogen generation was trapped at trap sites such as dislocation and dislocation loops, resulting in an increase of the hydrogen concentration. The concentration of hydrogen in Type 304 stainless steel Heats (A) and (C) was about 30 appm higher than the calculated hydrogen generation as shown in Fig. 7. The hydrogen concentration of 30 appm was comparable to that at the fluence of 1×10^{24} n/m² where hydrogen generation did not occur. This meant that hydrogen generated by nuclear transmutation was trapped at trap sites in Type 304 stainless steel and was not released by heating and γ irradiation.

The concentration of hydrogen in Type 304 stainless steel Heat (B) was higher than that in the other Heats at low fluence and increased with the increase of fluence. The reason is considered to be as follows. The nitrogen concentration in Heat (B) was higher than that in the other Heats (refer to Table 1). As described already, hydrogen was generated through the nuclear transmutation of nitrogen by neutron irradiation. Therefore, hydrogen concentration in Heat (B) was higher than that in the other Heats after irradiation. However, the difference was too large to be explained by this reason only. Another possible reason was that hydrogen was released by γ irradiation, but more hydrogen trapped at trap sites might have remained in Heat (B). As mentioned in Section 3.1, this could be assumed from the fact that the hydrogen concentration in unirradiated Heat (B) after heat treatment at 561 K was higher than that in the other Heats. A slight difference in the manufacturing process may also have an effect, because the manufacturers of Heats (A) and (C) and Heat (B) were different.

The trap sites such as irradiation-induced defects in Heat (B) were assumed to have more hydrogen than in the other Heats. It has also been reported that both hydrogen generated by corrosion and absorbed hydrogen are found on the surface of stainless steel [20]. Hydrogen from these two sources may be absorbed or trapped by the stainless steel. All such hydrogen would be counted in the hydrogen concentration.

3.3. SSRT results in Ar gas

The results of SSRTs are shown in Table 3, indicating that the total elongation and maximum stress are unchanged for the different fluences and strain rates. In

Table 3
SSRT results in Ar gas

Neutron fluence (n/m^2 , $E > 1$ MeV)	Strain rate (s^{-1})	Total elongation (%)	Max. stress (MPa)	%IG ^a
8.0×10^{25}	5×10^{-8}	9.5	891	0
		9.3	909	0
1.4×10^{26}	2.5×10^{-7}	9.3	896	0
		9.3	909	0
	5×10^{-8}	9.1	901	0
		9.2	893	0

^a Percent intergranular cracking of fracture surface.

addition, intergranular cracking was not observed. Typical fracture surfaces for different strain rates are shown in Fig. 8, which shows that no effect of strain rate is identified for the same neutron fluence.

No significant effect of neutron fluence, as seen in Table 3, should arise because mechanical properties like total elongation and maximum stress were saturated for such high neutron fluences. This tendency was the same as the results of high-temperature tensile tests of other irradiated materials, in general.

The results of SSRTs in high-temperature water of 20 ppb and 32 ppm DO for Type 304 stainless steel at the fluence of 1.4×10^{26} n/m^2 and strain rate of 2.5×10^{-7} s^{-1} that have been reported previously [8] as well as the results of this Ar test are shown in Table 4 and Fig. 9. The results at 32 ppm DO are also shown as a reference.

Comparing the results at 20 ppb DO with those of the Ar test, one of the two 20 ppb DO tests showed almost the same fracture strain and fracture pattern as the test in Ar whereas the other gave different results, i.e. a low fracture strain and percent intergranular cracking of fracture surface (9 %IG). The fact that intergranular (stress corrosion) cracking disappears at 200 ppb DO for unirradiated sensitized stainless steel [8], but intergranular cracking was found at 20 ppb DO for solution annealed stainless steels irradiated to 1.4×10^{26} n/m^2 , indicated the possibility of intergranular cracking caused by hydrogen.

On the other hand, Morisawa et al. [9] reported that sensitivity to hydrogen-induced intergranular cracking appeared when the fluence was increased, that the sensitivity increased with the increase of fluence, and that

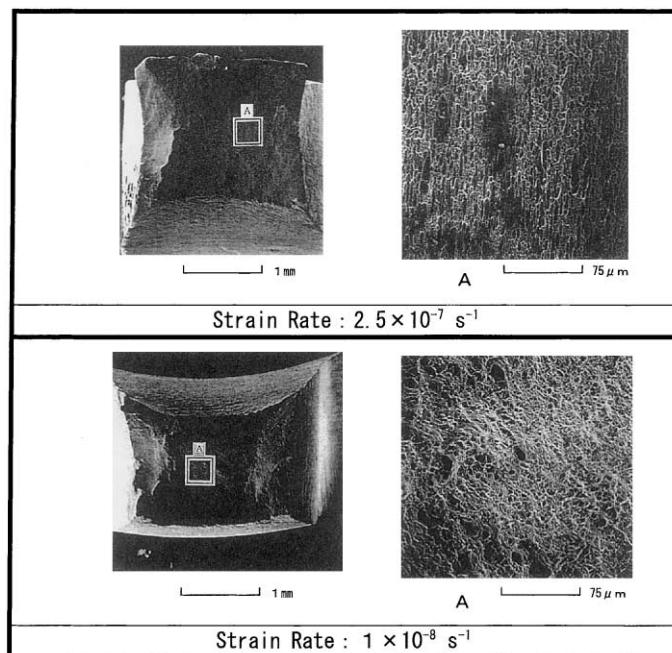


Fig. 8. SEM fractographs of irradiated Type 304 stainless steel tested in Ar gas. (Fluence: 1.4×10^{26} n/m^2).

Table 4
Comparison of SSRT results in Ar gas and in water at 561 K

Testing method	Neutron fluence (n/m^2 , $E > 1 \text{ MeV}$)	DO	Strain rate (s^{-1})	Total elongation (%)	Maximum stress (MPa)	%IG ^a
SSRT in Ar gas at 561 K ^b	1.4×10^{26}	–	2.5×10^{-7}	9.3	896	0
SSRT in water at 561 K [8]		20 ppb	2.5×10^{-7}	9.9	899	0
		32 ppm	2.5×10^{-7}	6.6	904	9
				6.4	872	95

^a Percent intergranular cracking of fracture surface.

^b This study.

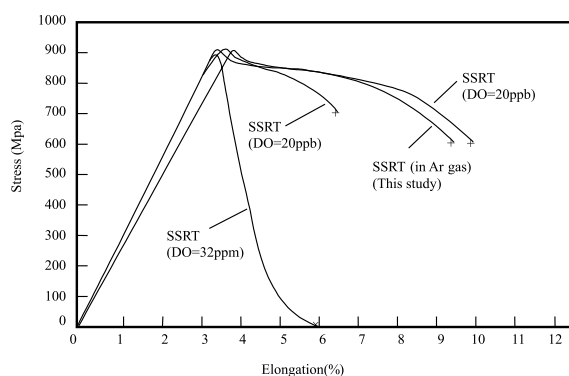


Fig. 9. Comparison of elongation-stress curves of SSRT results in Ar gas (this study) and in water [8] at 561 K. (Type 304 stainless steel, strain rate: $2.5 \times 10^{-7} \text{ s}^{-1}$).

average intergranular cracking depth was as deep as about 230 μm at the fluence as high as $1.4 \times 10^{26} \text{ n/m}^2$.

The hydrogen affecting the intergranular cracking of steel is the hydrogen in the steel and in the environment. In this study, the effect of hydrogen in steel was investigated. The concentration of hydrogen in the steel in Table 4 and Fig. 9 was estimated to be higher than 300 appm by extrapolation of the concentration obtained in this test. However, intergranular cracking was not observed in SSRTs in Ar gas. This meant that the hydrogen concentration was too small or hydrogen was

trapped in irradiation defects and so could not diffuse at this test temperature. If the hydrogen concentrations in this steel were higher or the test temperatures were higher, intergranular cracking could possibly have appeared.

A comparison of the literature data on tensile tests for irradiated 10% cold-worked Type 304 stainless steels [10] with those of this test is made in Table 5. The SSRTs in Ar at 581 K for Type 304 stainless steel irradiated in a PWR showed intergranular cracking at the fluence of $5.0 \times 10^{25} \text{ n/m}^2$ and strain rate of $1 \times 10^{-6} \text{ s}^{-1}$, and as the strain rate decreased, the %IG increased. The differences between the two cases included irradiation conditions such as irradiation temperature and pressure, water quality (irradiated in a PWR vs. a BWR), with or without cold working, and test temperature (588 K or 561 K). At higher temperatures, the diffusivity of hydrogen is increased [21] and hydrogen trapped in trap sites may become mobile due to the movement of dislocations by tensile stress.

Other literature results of SSRTs in Ar for steel irradiated with neutrons after sensitization are shown in Table 6 [22]. Intergranular cracking was not observed for unirradiated sensitized Type 304 stainless steel, but when irradiated, sensitized Type 304 stainless steel showed intergranular cracking (5 %IG) at the relatively low fluence of $3 \times 10^{23} \text{ n/m}^2$ in SSRT in Ar. The observations with a transmission electron microscope and the measurements of the reactivating rate by a

Table 5
Comparison of SSRT results in Ar [10]

	Material	Neutron fluence (n/m^2)	Test temperature (K)	Strain rate (s^{-1})	Total elongation (%)	Max. stress (MPa)	%IG ^a
Ref. [10]	Type 304 ^b	5.0×10^{25}	588	5.0×10^{-4}	8.0	924	0
				1.0×10^{-6}	9.3	944	3–4
				2.0×10^{-7}	9.0	865	15–20
				1.0×10^{-8}	9.3	848	30–35
This test	Type 304	8.0×10^{25}	561	5×10^{-8}	9.3	909	0
				2.5×10^{-7}	9.3	896	0
				1×10^{-8}	9.2	893	0

^a Percent intergranular cracking of fracture surface.

^b 10% cold-worked tubing.

Table 6

Literature data of SSRT in Ar for stainless steel irradiated with neutrons after sensitization [22]

Material	Fluence (n/m ²)	DO ^a (ppm)	YS ^b (MPa)	UTS ^c (MPa)	Total E ^d (%)	%IG ^e (%)	%TG ^f (%)	Dimple (%)	
Sensitized Type 304	0	<0.01	19.1	41.8	34.0	0	44	56	
			18.9	43.2	30.0	0	47	53	
	3 × 10 ²³	<0.01	Ar	18.4	50.2	45.5	0	0	100
				27.4	40.6	13.6	14	28	58
				27.1	41.1	16.1	19	15	66
Solution heat- treated Type 304	0	8	27.4	48.5	37.3	5	0	95	
			13.6	41.0	37.1	0	0	100	
	3 × 10 ²³	8	26.0	47.5	35.3	0	0	100	

^a Dissolved oxygen.^b Yield strength.^c Ultimate tensile strength.^d Total elongation.^e Percent intergranular cracking of fracture surface.^f Percent transgranular cracking of fracture surface.

electrochemical potentiokinetic reactivation (EPR) method indicated no difference in the microstructure or corrosion resistance. The intergranular cracking observed in SSRTs is considered to be caused by both mechanical cracking and SCC [22], but not by hydrogen.

Intergranular cracking was observed in the SSRTs in Ar for steel irradiated after cold working or sensitization, but was not observed for the Type 304 stainless steel irradiated after solution heat treatment as in this experiment. The change of microstructure in stainless steel by cold working or sensitization before irradiation seemed to have affected the appearance of intergranular cracking by SSRTs in Ar after irradiation.

4. Conclusions

The concentration of hydrogen in steel was measured and SSRTs in Ar were carried out for Type 304 stainless steel irradiated up to the fluence of 8×10^{23} to 1.4×10^{26} n/m² in a BWR.

The following conclusions were drawn:

1. The concentration of hydrogen in unirradiated Type 304 stainless steel was 160–220 appm for AR steels and 50–70 appm for steel heat-treated at 561 K × 72 h.
2. The concentration of hydrogen in irradiated Type 304 stainless steel decreased at low fluence (below 5×10^{24} n/m²) and then increased with the increase of fluence. The first decrease was considered due to the release of hydrogen by heating and γ irradiation at the early stage of reactor operation.
3. The hydrogen concentration at higher fluence (higher than 5×10^{24} n/m²) in Type 304 stainless steel was equal to or larger than the sum of the hydrogen con-

centration remaining at lower fluence and hydrogen generation calculated based on the fluence irradiated to Type 304 stainless steel. Therefore, the increase of hydrogen concentration was considered due to the hydrogen generated by nuclear transmutation.

4. Intergranular cracking was not observed in the SSRT in Ar at the fluence as high as 1.4×10^{26} n/m² and very low strain rate of 1×10^{-8} s⁻¹. This meant that either the hydrogen concentration was too small, or hydrogen was trapped in irradiation defects, and unable to diffuse at the test temperature.

References

- [1] M. Kodama, R. Katsura, J. Morisawa, S. Nishimura, S. Suzuki, K. Asano, K. Fukuya, K. Nakata, in: Proceedings of the Sixth International Symposium on Environmental Degradation of Materials in Nuclear Power Systems – Water Reactors, San Diego, CA, August 1993, p. 583.
- [2] H.M. Chung, W.E. Ruther, J.E. Sanecki, T.F. Kassner, in: Proceedings of the Sixth International Symposium on Environmental Degradation of Materials in Nuclear Power Systems – Water Reactors, San Diego, CA, August 1993, p. 511.
- [3] M. Kodama, S. Nishimura, J. Morisawa, S. Shima, S. Suzuki, M. Yamamoto, in: Proceedings of the Fifth International Symposium on Environmental Degradation of Materials in Nuclear Power Systems – Water Reactors, Monterey, CA, August 1991, p. 948.
- [4] P.L. Andresen, F.P. Ford, S.M. Murphy, J.M. Parks, in: Proceedings of the Fourth International Symposium on Environmental Degradation of Materials in Nuclear Power Systems – Water Reactors, Jekyll Island, GA, August 1989, p. 83.
- [5] W.L. Clarke, A.J. Jacobs, in: Proceedings of the First International Symposium on Environmental Degradation

- of Materials in Nuclear Power Systems – Water Reactors, Myrtle Beach, SC, August 1983, p. 451.
- [6] K. Asano, S. Nishimura, Y. Saito, H. Sakamoto, Y. Yamada, T. Kato, T. Hashimoto, in: Proceedings of the Fifth International Symposium on Environmental Degradation of Materials in Nuclear Power Systems – Water Reactors, Monterey, CA, August 1991, p. 838.
- [7] D.I.R. Noris, C. Baker, J.M. Titchmarch, in: Proceedings of the Symposium on Radiation-Induced Sensitization of Stainless Steel Held at Berkeley Nuclear Laboratory, CEGB, September 1986, p. 86.
- [8] M. Kodama, R. Katsura, J. Morisawa, S. Nishimura, S. Suzuki, K. Takamori, S. Shima, T. Kato, in: Proceedings of the Seventh International Symposium on Environmental Degradation of Materials in Nuclear Power Systems – Water Reactors, Breckenridge, CO, August 1995, p. 1121.
- [9] J. Morisawa, M. Kodama, S. Nishimura, K. Asano, K. Nakata, S. Shima, J. Nucl. Mater. 212–215 (1994) 1396.
- [10] M.P. Manahan, R. Kohli, Invited Paper, Ninth International Conference on Structural Mechanics in Reactor Technology, 1987, p. 75.
- [11] D.I. Garner, R.R. Kensey, BNL-325, 3rd Ed., vol. II, Neutron Cross-Sections, 1976.
- [12] L.R. Greenwood, J. Nucl. Mater. 115 (1983) 137.
- [13] K. Ebihara, Chemical Handbook Basis Volume, Rev. 3, Chemical Institute of Japan, 1984, p. II-71.
- [14] K. Asano, S. Nishimura, Y. Saito, H. Sakamoto, Y. Yamada, T. Kato, H. Hashimoto, J. Nucl. Mater. 264 (1999) 1.
- [15] H. Farrar, B.M. Oliver, J. Vac. Sci. Technol. A 4 (1986) 1740.
- [16] M. Hasegawa, M. Oosawa, A. Natori, Tetsu-to-Hagane 65 (1979) 1213.
- [17] Radiation Shielding Information Center Computer Code Collection, CCC-371/ORIGEN-2.
- [18] M. Touge, T. Miki, M. Ikeya, K. Kamachi, J. Jpn. Inst. Met. 46 (3) (1982) 341.
- [19] N. Yoshida, N. Ashizuka, T. Fujiwara, T. Kurita, T. Muroga, J. Nucl. Mater. 155–157 (1988) 775.
- [20] H. Anzai, J. Kuniya, E. Kikuchi, N. Ohnaka, in: Proceedings of the Fourth International Symposium on Environmental Degradation of Materials in Nuclear Power Systems – Water Reactors, 1989, p. 104.
- [21] Y. Sakamoto, H. Katayama, J. Jpn. Inst. Met. 46 (8) (1982) 341.
- [22] K. Hide, T. Onchi, M. Mayuzumi, K. Dohi, Y. Futamura, Corrosion 51 (1995) 757.